Please Note:

The following document has been left in its original state and may contain outdated contact information.

Please be advised of the current contact information for Microcosm, Inc.:

401 Coral Circle

El Segundo, CA 90245-4622

Phone: (310) 726-4100

FAX: (310) 726-4110

website: www.smad.com

general e-mail:
microcosm@smad.com

AUTONOMOUS CONTROLLED LANDING ON COMETARY BODIES

SIMON DAWSON, CURTIS POTTERVELD, HANS KÖNIGSMANN, LEO EARLY

AUTONOMOUS CONTROLLED LANDING ON COMETARY BODIES

Simon Dawson, Curtis Potterveld, Hans Königsmann, Leo Early*

A simulation environment is developed that will propagate a controlled orbit about asteroid and cometary bodies in the solar system. This simulation allows as input the location and orbit of the central body, and includes models for the gravitational field, continuous atmospheres, and outgassing jets. The simulation is based on Microcosm's High-Precision Orbit Propagator, and can be used for a variety of mission analyses.

Control algorithms for autonomous controlled landing on a cometary body were developed. These algorithms will guide the spacecraft though a series of predetermined waypoints down to the surface of the comet. A control module was integrated into a simulator to implement these algorithms. The controller was then tested under a variety of situations. The algorithms maintained control of the spacecraft at all times and achieved the desired spacecraft end state to a high degree of accuracy.

INTRODUCTION

Interest in exploring and studying small bodies, comets, and asteroids has led to several successful encounters with these bodies, such as those by Giotto, Galileo, and NEAR. Currently proposed missions, like NASA's Champollion/DS4 project, and SpaceDev's commercial deep-space ventures, are calling for rendezvous with, and sample-return from, these bodies. Such missions would benefit greatly from spacecraft with the ability for autonomous trajectory control, especially during the proximity operations, landing, and departure phases of the mission.

During such mission phases the large time delays associated with ground control may become prohibitively risky. Also the need for round-the-clock coverage from the Deep Space Network could become a resource issue (scheduling and cost). Giving the spacecraft the ability to autonomously control its own landing, and possible rendezvous with the return vehicle for sample-return scenarios, could simplify and reduce the overall cost of the mission as well as increase overall reliability. This paper presents some results from initial simulations of autonomously controlled descent and landing on a cometary nucleus.

These simulations were executed on a modified version of Microcosm's commercially available High Precision Orbit Propagator (HPOP). This modified propagator allows the user to completely specify the state of the desired central body, including its position and orbit in the solar system, its attitude and rotation rate, as well as its size, and coefficients for a spherical expansion describing its gravity potential. The user can also specify the atmosphere, if any, and in the case of a cometary body any active jets coming off the surface. With this propagator most comet or asteroid models supplied by the science community can be used in the simulation. An additional module was integrated into HPOP to implement the control algorithms, and apply the calculated ΔV.

The cometary body model used in the simulation in this work was an amalgam of the models described in the literature. The size and radius of the comet were taken from Möhlmann's[1] work on comet 46 P/Wirtanen. The atmosphere and jets are based on the work of Oria[2] and Klinger[3]. The gravity potential field was based on the work of Miller[4]. Other models are anticipated to be used in any future work.

---

* Technical Staff, Microcosm, Inc. 2377 Crenshaw Blvd. #350, Torrance, CA 90501, (310) 320-0555
email: sdawson@smad. com, or cpotterveld@smad.com

The control algorithms are based on a simple state-feedback controller. A series of waypoints were calculated, consisting of state vectors and associated time tags, which guide the spacecraft on a close approach and landing trajectory. The spacecraft travels from waypoint to waypoint adjusting its state vector to meet the each waypoint at the appropriate time. The difficult problem of autonomous navigation was considered to be outside the scope of this current investigation, and will be tackled in future investigations. Thus in these preliminary simulations the navigation solutions given to the control algorithms contain no error sources. In light of this, the results obtained must be taken as a qualitative and not quantitative assessment of the controller performance.

The next section this paper outlines in more detail the abilities of the orbit propagator to implement the cometary models. It also provides more information on the comet model used in the simulations, and presents results of simulated, controlled trajectories.

SIMULATION ENVIRONMENT

Central Body Location and Gravity Model

HPOP allows uses to specify the location and orbit of the planetary body to use as the central body for the propagation. The central body is assumed to have an unperturbed Keplerian elliptical orbit and its position is determined by evaluating the standard Keplerian-to-Cartesian element transformation. The user is required to supply as input the following Keplerian orbit elements and the epoch at which they are valid:

a	semi-major axis
e	eccentricity
i	inclination
Ω	longitude of ascending node
ω	argument of periapsis
M	mean anomaly

The angular elements refer to the mean ecliptic and equinox of the standard epoch J2000.0.

The standard Keplerian-to-Cartesian element transformation[5] is used in the program, with the exception of the solution to Kepler's Equation, which is obtained by using the following enhanced algorithm where E is the eccentric anomaly:

$$\Delta M = \frac{e \sin M}{1 - e \cos M}$$

$$E \leftarrow \begin{cases} M - 1 & \text{if } \Delta M < -1 \\ M + \Delta M & \text{if } -1 < \Delta M < 1 \\ M + 1 & \text{if } 1 < \Delta M \end{cases}$$

$$E \leftarrow E + \frac{M - E + e \sin E}{1 - e \cos E} \qquad \text{until converged}$$

This algorithm is guaranteed to converge for all M and all $e < 1$, and is sufficiently fast.

The user is also required to supply as input the values of these quantities and the central-body rotation rate, W, at the epoch given for the central-body orbit elements. The right ascension and declination must be referred to the mean Earth equator and equinox of J2000.0 and the longitude of the prime meridian must be referred to the ascending node of the central-body equator on the Earth's equatorial plane. The angles must be given in degrees and the rotation rate in degrees/day.

Once the values of α, δ, and W are known, the attitude matrix $\bar{\bar{\mu}}$ of the central body is given by:

$$\bar{\bar{\mu}} = \bar{\bar{R}} \cdot \bar{\bar{I}} \cdot \bar{\bar{N}}$$

where:

$$\bar{\bar{R}} = \begin{bmatrix} \cos W & \sin W & 0 \\ -\sin W & \cos W & 0 \\ 0 & 0 & 1 \end{bmatrix} \quad \text{Rotation}$$

$$\bar{\bar{I}} = \begin{bmatrix} 1 & 0 & 0 \\ 0 & \sin\delta & \cos\delta \\ 0 & -\cos\delta & \sin\delta \end{bmatrix} \quad \text{Inclination}$$

$$\bar{\bar{N}} = \begin{bmatrix} -\sin\alpha & \cos\alpha & 0 \\ -\cos\alpha & -\sin\alpha & 0 \\ 0 & 0 & 1 \end{bmatrix} \quad \text{Node}$$

Only the central body will use a spherical harmonic expansion for the gravity field. All other third-body masses in the simulation are assumed. to behave as point masses. The acceleration caused by the central-body gravitational field is computed[5], but modified to use normalized instead of unnormalized gravity model coefficients. The acceleration caused by third-body point-mass gravity fields and by solar radiation pressure is also computed[5].

The solar radiation pressure model is the same for all central bodies except the Sun, which has no shadow. Bodies other than the Sun have circular, cylindrical shadows with sharp edges pointed directly away from the Sun.

Atmospheric Drag Model

The acceleration caused by atmospheric drag is given by:

$$\bar{a} = -\frac{C_D A}{M} \frac{\rho}{2} \left| \bar{v} - \bar{v}_A \right| \left(\bar{v} - \bar{v}_A \right)$$

where:

$\bar{r}$	=	position of spacecraft
$\bar{v}$	=	velocity of spacecraft
$\bar{a}$	=	acceleration of spacecraft
C_D	=	coefficient of drag of spacecraft
A	=	cross-sectional area of spacecraft
M	=	mass of spacecraft
ρ	=	density of atmosphere
$\bar{v}_A$	=	velocity of atmosphere

Then the atmosphere density is given by:

$$\rho = \rho_0 \, e^{\frac{h_0 - h}{s}} \left(\frac{R + h_0}{R + h} \right)^2$$

where

h	=	height of spacecraft above reference ellipsoid of central body
h_0	=	reference height of atmosphere model
s	=	scale height of atmosphere model
ρ_0	=	reference density of atmosphere model

The user is required to supply the last three parameters as input. If the central body is a comet, the same expression gives the density of the continuous component of the atmosphere (the region outside all jets).

The factor

$$\left(\frac{R + h_0}{R + h}\right)^2$$

was included in the model to take into account the fact that comets have very large scale heights s while conservation of matter indicates that an atmosphere flowing outward with constant speed cannot have the same density everywhere. An attempt to justify this factor by deriving a more rigorous atmosphere model correct for spherical bodies failed.

The atmosphere velocity is given by:

$$\bar{v}_A = \frac{R^2}{r^2}\,\bar{\omega} \times \bar{r}$$

This assumes that:

1. The atmosphere at radial distance R co-rotates with the central body.
2. Angular momentum is conserved as the slowly outgassing atmosphere recedes from the central body.
3. Angular momentum is not transferred between concentric spherical shells of atmosphere.

Outgassing Jet Model

The surfaces of active comets are spotted with outgassing jets which spew matter into the interplanetary medium at speeds of up to 2 km/sec. The jet model used in HPOP assumes that the central body is a sphere, that jets are conical with sharp edges, that the jet density is constant over a spherical shell centered at the apex of the jet cone and varies inversely as the square of the distance from the apex, and that the jet speed remains constant throughout the jet cone. This is equivalent to assuming that the gas in the jet expands horizontally at a constant rate as it flows outward but does not expand vertically. The cone axis is assumed to point directly away from the center of the central body, although the cone apex is not required to be at the center. The geometry of the jet is shown below.

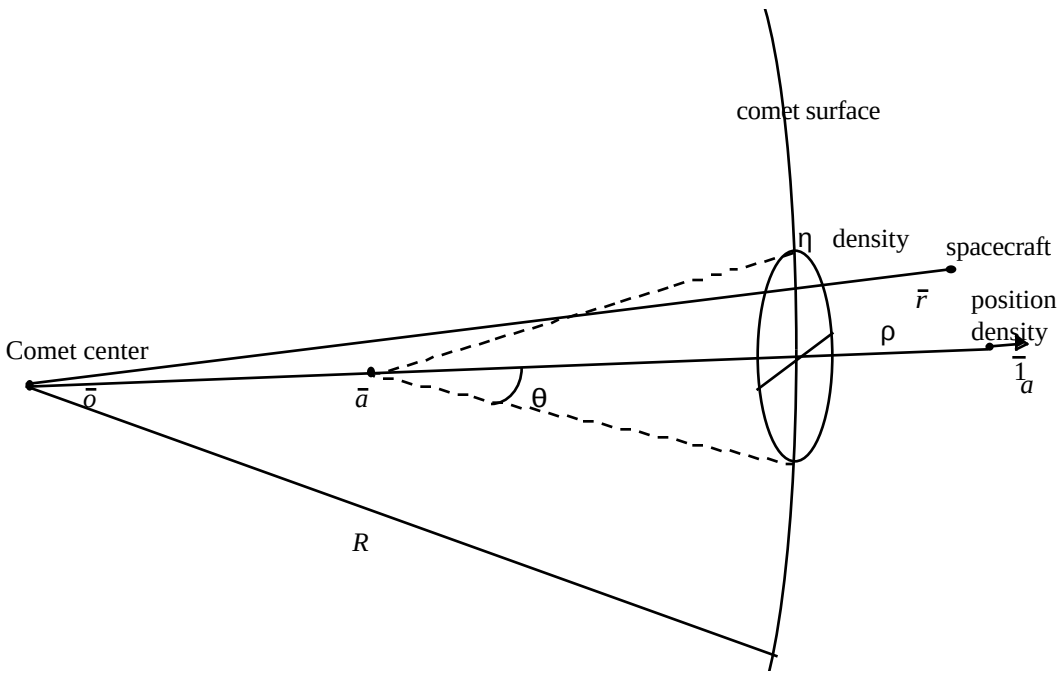

Figure 1. Geometry of the Cometary Jet as Defined in the Cometary Environment Model

The user is required to supply the following quantities as input for each defined jet

λ	longitude of jet center
φ	latitude of jet center
θ	jet cone angle
Γ	jet cone radius at surface of central body
η	jet density at edge of cone and surface of central body
V	jet speed

The longitude and latitude of the jet center must be given in the body-fixed reference frame, and all angles must be given in degrees.

ρ and $\bar{v}_A$ become singular as the cone angle approaches zero, as it would for a cylindrical jet. It is therefore convenient to define an auxiliary vector $\bar{c}$ which is always well-defined and give the results in terms of that. The vector 1_a which appears in the derived expression for $\bar{c}$ is the unit vector from the center of the comet to the center of the jet cone on the surface and is given by:

$$\bar{1}_a = \bar{\bar{\mu}}^T \cdot \begin{bmatrix} \cos\lambda \cos\varphi \\ \sin\lambda \cos\varphi \\ \sin\varphi \end{bmatrix}$$

where $\bar{\bar{\mu}}$ is the attitude matrix of the comet. Modifying these expressions to take into account the rotation of the central body yields the expressions shown on the attached sheets labeled “Rotating Surface Jets”, which are used in the program.

The current jet model contains many inaccuracies which will be addressed in future efforts:

1. The model assumes that the central body is a sphere. Real comets which have been observed are shaped more like potatoes than spheres.
2. The model assumes that the jet density is constant across the width of the jet and drops suddenly to zero at the edge. Real jets will be densest in the center, with density falling off smoothly as you approach the edge. Oria[2] assumes a Gaussian distribution, which is probably closer to the truth.
3. The model assumes that the jet speed is the same in all parts of the jet, which implies that the jet density varies inversely as the square of the distance from the cone apex. In real jets, the speed is greatest near the center and falls off smoothly as you approach the edge, although the slope may be very large near the edge. In addition, the jet speed increases dramatically as the jet recedes from the comet due to hydrodynamic expansion of the gas. For a water-rich comet at about 4 AU from the Sun, the speed of the jet increases from about 300 m/s at the surface to a terminal speed of 1-2 km/s some distance away[2]. The increase in speed brings about a corresponding drop in density due to conservation of matter.
4. The model assumes that the cone axis of the jet points directly away from the center of the comet. Real comets being potato-shaped, the center is not that well defined, and the jets are probably more or less perpendicular to the local surface instead of being directed away from the center of mass.
5. The position model for jets on a rotating comet assumes that the jets rotate with the comet as if the comet-jet assembly were a rigid body, while the velocity model takes into account the conservation of angular and linear momentum as the jets recede from the comet. The position and velocity models are thus inconsistent with each other. This is good enough for investigating the general nature of spacecraft trajectories near active comets, but it will not do for planning maneuvers near a real body. In reality, the jets will trace out spiral patterns as they recede from the comet nucleus. Since different jets may have different speeds, the patterns can get quite complicated at large distances.
6. The model assumes that when two jets overlap, the accelerations caused by each add vectorially. In reality, when two jets impinge near the surface of the comet, a shock front probably forms between them. At very large distances, the jets may lose their separate identities and merge gradually into the general cometary atmosphere.

COMET MODEL

Gravity Model

In the preparation of the results during this study two variants of the cometary nucleus’ gravity field were used. The first one was a very simple 8 x 8 field, its coefficients were simply random numbers between zero and one. This first field was used as a check on the validity of the simulation.

A more ‘useful’ field was produced that largely followed the work detailed in Miller[4], that is an attempt to more closely mimic our best estimate of what a cometary gravity field may look like. This field is a 6 x 6 field and is based on the data in the table below and normalized:

Table 1. Gravitational Harmonics of the Hypothetical Cometary Nucleus

Gravity Harmonics				
μ (km^3/s^2)	30×10^{-9}			
C_{20}, C_{22}	– 0.500	+ 0.140		
C_{40}, C_{42}, C_{44}	+ 0.053	– 0.032	+ 0.00070	
C_{60}, C_{62}, C_{64}, C_{66}	– 0.072	+ 0.021	– 0.00014	+ 0.000056

To first order, the nucleus is a prolate spheroid. In future efforts the addition of MasCons would certainly be high on the agenda for environmental modeling improvements.

The solar radiation pressure force is modeled using the user-defined Keplerian orbital elements to produce a comet to Sun distance and direction. This coupled with the information the user supplies on the rotation axis direction and the rate of rotation to calculate the solar radiation pressure as described in the Simulation Environment section.

The Bulk atmosphere of the Comet & The Modeling of 'Jets'

The comet's surface outside of the jets is not wholly inactive. The residual outgassing of the bulk surface produces a low density atmosphere surrounding the nucleus. Since the surface is at a lower temperature than the active jets then the sublimation rate is much reduced. This effect can be seen in Figure 2.

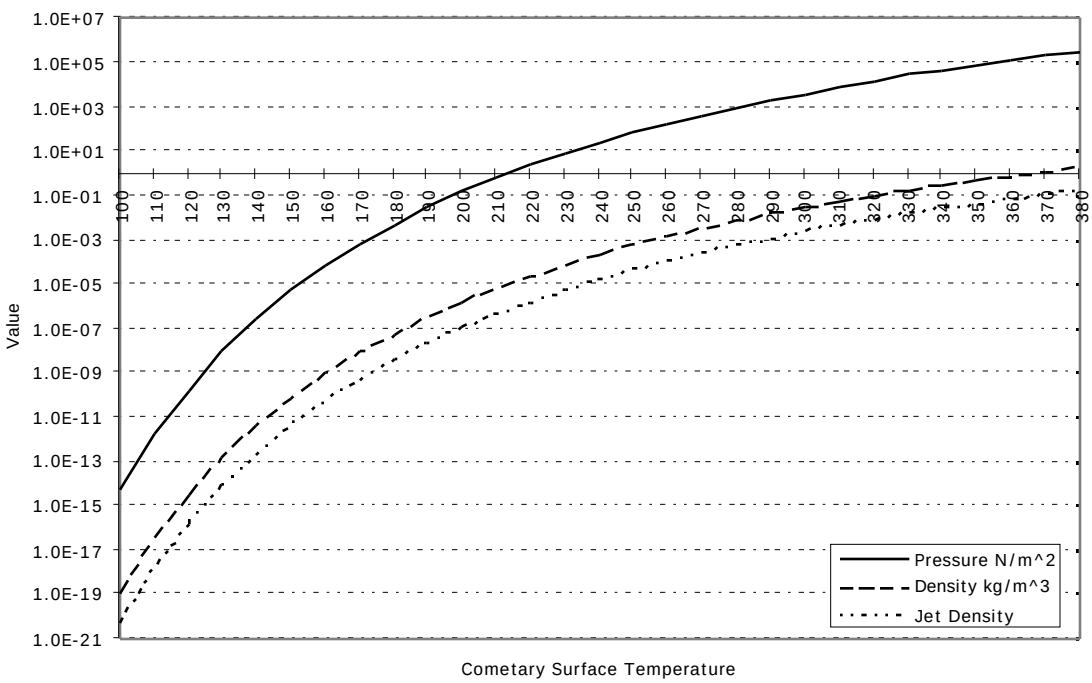

Figure 2. Cometary Nucleus Bulk Atmosphere and Jet Density vs. Temperature

Several assumptions went into the production of the data shown in Figure 2. The characteristic jet velocity has been set at 350 m/s[2,3]; a compromise value between the extremes to be found in the literature. The gravitational acceleration at the surface of the comet used was 6.12×10^{-5} m/s^2. This equates to a

comet of mass 5.75 10^{11} kg and radius 700 m. These assumptions are largely modeled after Möhlmann's [1] work on modeling Comet 46 P/Wirtanen and are, in fact, consistently used throughout the simulations of the spacecraft motion about the nucleus and the cometary environment.

For the actual trajectories about the nucleus a bulk surface temperature of 130 K and an active region, that is a jet, temperature of 220 K were used. These temperature values again are approximate averages of values shown in the literature for similarly sized comets. In addition, the jet sublimation rate was reduced by a 'muck-to-ice' fraction of 20% after Möhlmann[1]. The pressure curve shown in Figure 2 is representative of the pressure in the bulk atmosphere assuming ideal gas behavior.

COMET LANDING CONTROLLER

The basic approach behind the comet controller was to take a waypoint guidance scheme as the desired trajectory – a trajectory that is physically possible for an unperturbed ballistically moving object – and treat the comet's atmosphere, jets, non-point-mass gravity field, the Sun's tidal and radiation pressure acceleration as merely perturbations. The perturbations to the ballistic, or Keplerian, trajectory would therefore be actively removed by the action of the controller working through the spacecraft's propulsion system.

A mathematical model of the spacecraft dynamics has been developed using state-space methods, and the actual controller is a regulator using full state feedback. Appropriate gains have been found using pole-placement. Our approach was to develop a simple controller and verify the linear analysis with a software simulation before proceeding to more complex controllers. Realistic non-linearities were introduced, such as finite thrust and delays, however, other simplifications have been used throughout this work and must be addressed in future efforts, such as:

1. Navigation system error and biases
2. Estimation of missing states, using appropriate filters and observers
3. Comet rotation and surface properties, which might require implementation of a "hold-down" mode
4. Comet contamination issues with respect to thruster plume
5. Autonomous way-point generation (see below)

The basic unperturbed trajectory was produced using a solution of Lambert's Problem using Universal Variables[6]. The baseline trajectory solved for initially was the minimum energy Lambert Problem solution. This trajectory's time interval, Δt, was then varied in a step-like fashion, above and below the baseline Δt, so as to produce many trajectories when these Δt's were 'fed' to the Universal Variables solver. Out of these many trajectories a single one was chosen to represent a moderately good trade among time of transfer, Δv requirements at start and end, and avoidance of cometary jets. This trade was performed in a qualitative manner; it is planned that a more automated approach to this problem may be available as a part of future development of this tool. A representative plot of some waypoints and their associated trajectories is shown in Figure 3.

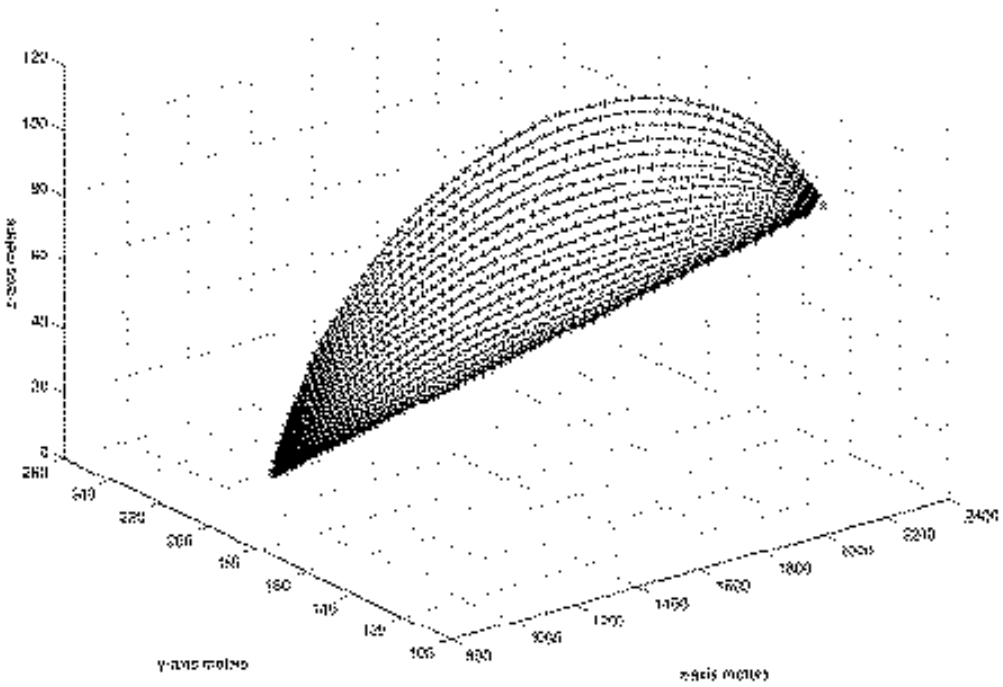

Figure 3. Representative Trajectories and their Associated Waypoints for Comet Landings

State feedback gains where derived to control an 87kg satellite. The gains where chosen to provide a stable controller, with a reasonable response time (~20 to 30 sec). Between any two waypoints, the desired spacecraft state was determined by a linear interpolation of the neighboring waypoints.

The time between any two waypoints was determined by dividing the distance between the waypoints by the average velocity at the waypoints. While not entirely accurate for a ballistic trajectory, the scheme is easy to implement and sufficient for the preliminary study.

INITIAL SIMULATIONS AND RESULTS

Initial simulations were performed for a small cometary body. The body was assumed to have the following characteristics:

Table 2. Nucleus Characteristics Used in Landing Simulation

$\mu = 30\ m^3/s^2$	Radius = 700 m
Rotation period = 6 hr	Scale height = 7.6×10^8 m
An exponentially decaying atmosphere of reference density, $1.5 \times 10^{-13}\ kg/m^3$	

The placement of jets and their activity depended on the particular simulation being run, but when active were given the following characteristics:

Table 3. Jet Characteristics Used in Landing Simulations

Velocity v at surface	350 m/s	Cone 1/2 angle	30°
Density ρ at surface	1.75×10^{-6} kg/m^3		

Waypoints were generated to bring a satellite from a state vector resembling a circular orbit at 20 km to a close approach at 750 m. For convenience sake, the spacecraft approach trajectory was initiated on the comets arbitrarily defined x-axis – the z-axis being defined as the nucleus' rotation axis – and made its closest approach when it crossed the y-axis. Figure 4 shows the location of the waypoints relative to the comet.

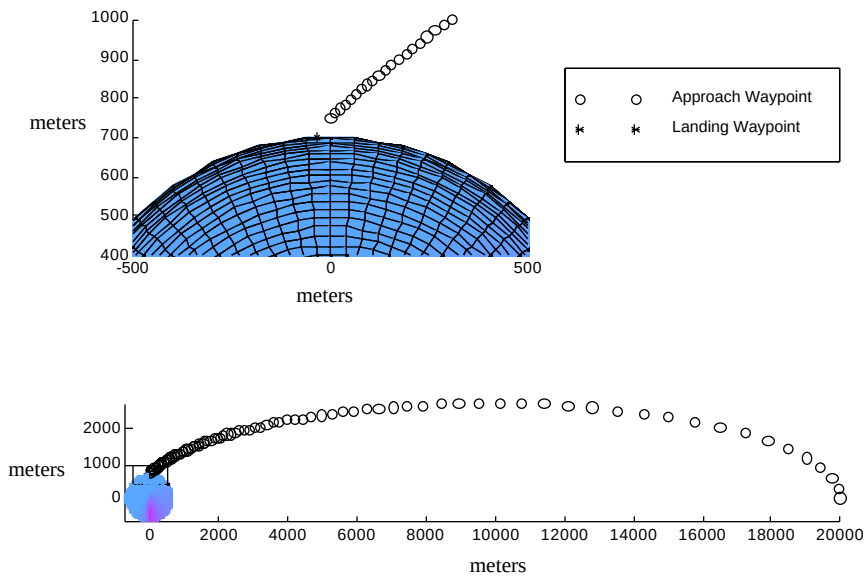

Figure 4. Baseline Trajectory and Waypoints

An initial simulation was run as a baseline for comparing the stability of the controller under various perturbations. The simulation parameters were the same as those used in calculating the waypoints, and had no active jets or perturbing bulk atmosphere. The comet was given random gravity perturbations for its gravity model; however, for this simulation the comet body was not rotating. Figure 5 shows the results of this simulation. The spacecraft successfully followed the waypoints down to 750 m. The spacecraft ended its controlled trajectory 3.02 m and 0.12 m/s off from the final waypoint, using only 0.047 m/s of ΔV.

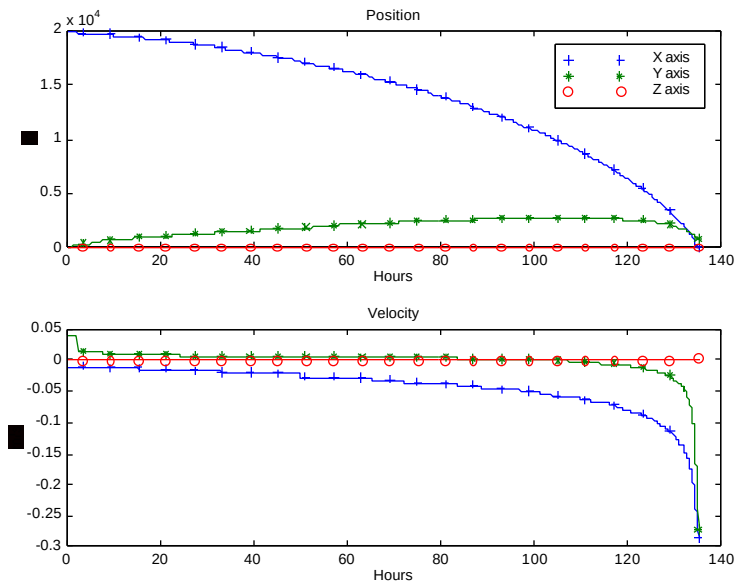

Figure 5. Position and Velocity Plots vs. Time for Baseline Comet Landing

A major contribution to these offsets may be the timing method for the waypoints. Since the timing method was not ballistic, especially near the comet, the spacecraft will drift off the planned trajectory. The controller will work to keep it on the trajectory. The offsets are within the expected bias response of the controller.

Several simulations were run to determine the sensitivity of the orbit controller to various perturbations in the model. The following table and Figures 6 to 15 summarize the perturbations and results of the simulation.

Table 4. Comet Landing Simulation Perturbations and Results (Results from Run #8 shown graphically in Figure 13).

Baseline	No Atmosphere, No Jets, No Rotation, No offset in initial pos & vel	random gravity field	Distance Error 3.02 m	Velocity Error 0.12 m/s	ΔV used 0.047 m/s
Run #	**Perturbation from Baseline** *(in terms of initial position & velocity or comet characteristic)*	**Gravity Field 'Make-up'**	**Distance Offset from Baseline (m)**	**Velocity Offset from Baseline (m/s)**	**ΔV used (m/s)**
1	1.5 × initial pos & vel	random coefficients	0.01	0	23.394
2	0.5 × initial pos & vel	random	0.01	0	22.646
3	1.1 × initial pos & vel	random	0.01	0	5.109
4	0.9 × initial pos & vel	random	0.01	0	4.715
5	2 × μ	random	–0.04	0	0.071
6	0.5 × μ	random	0.05	0	0.035
7	Rotating body & 1 × μ	random	–0.03	0	0.043
8	Atm & jet held on x-axis	realistic	2.39	–0.03	34.05
9	Atm & jet held on y-axis,	realistic	0.01	0	0.433
10	Atm & rotating jet (starting on x-axis)	realistic	0.01	0	6.41

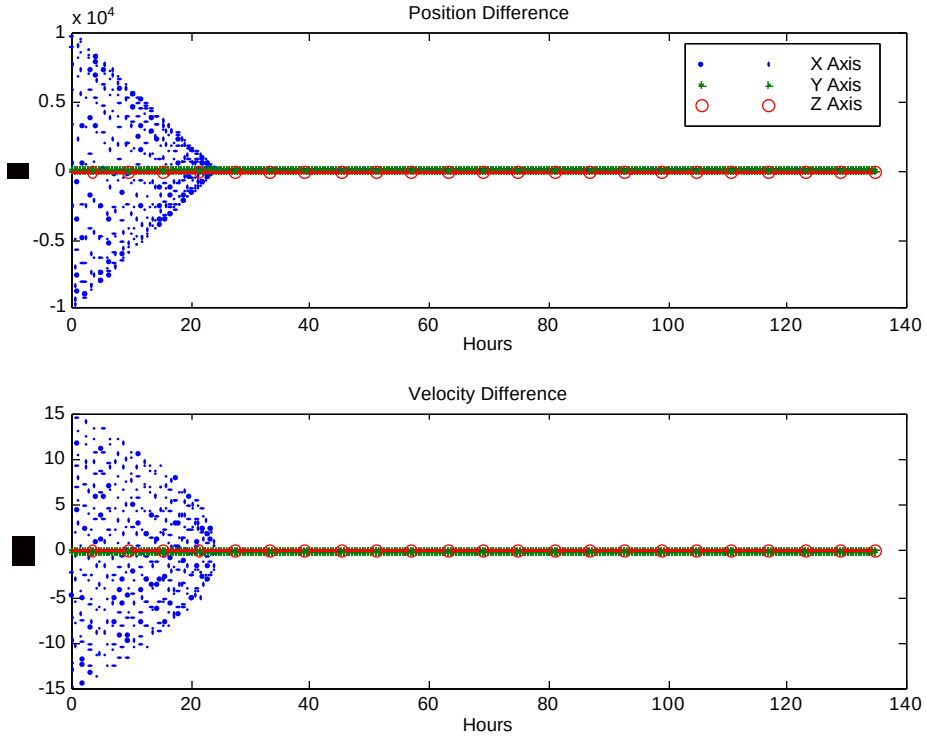

Figure 6. Position and Velocity Differences from Baseline: Initial Position and Velocity Values 150% of Baseline Values (Run #1)

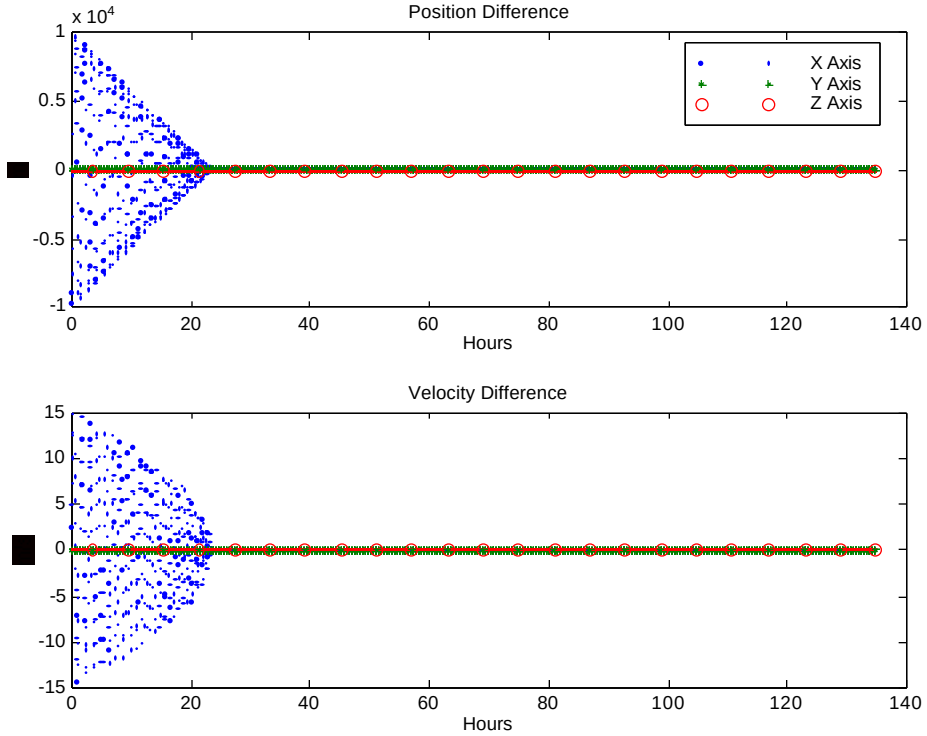

Figure 7. Position and Velocity Differences from Baseline: Initial Position and Velocity Halved from Baseline Values (Run #2)

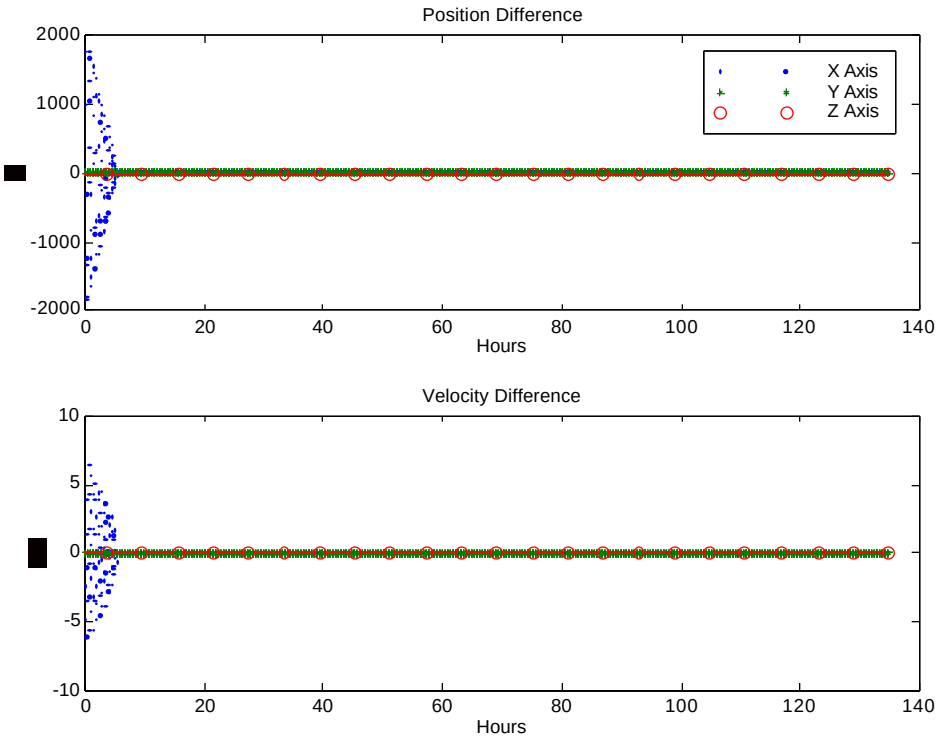

Figure 8. Position and Velocity Differences from Baseline: Initial Position and Velocity 110% of Baseline Values (Run #3)

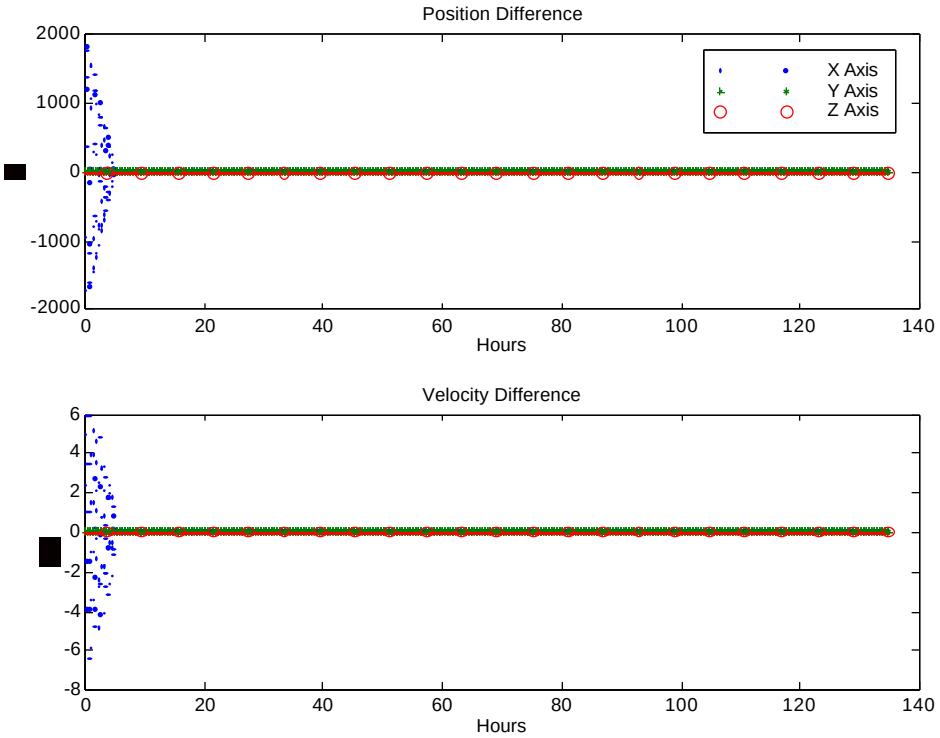

Figure 9. Position and Velocity Differences from Baseline: Initial Position and Velocity 90% of Baseline Values (Run #4)

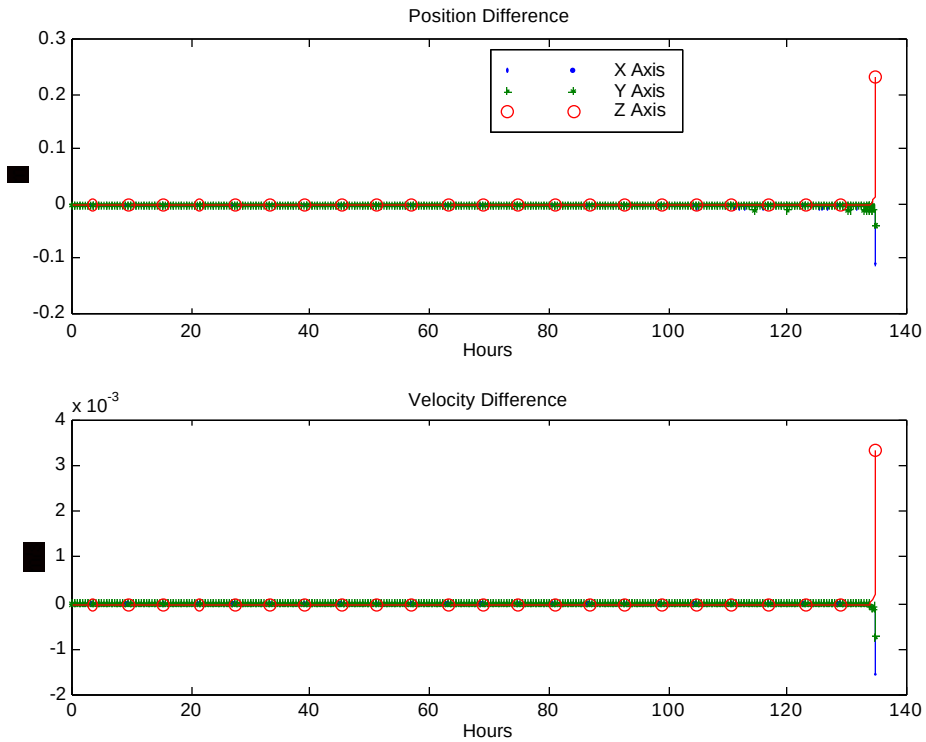

Figure 10. Position and Velocity Differences from Baseline: Cometary Gravitational Parameter, μ, Doubled Over Baseline Value (Run #5)

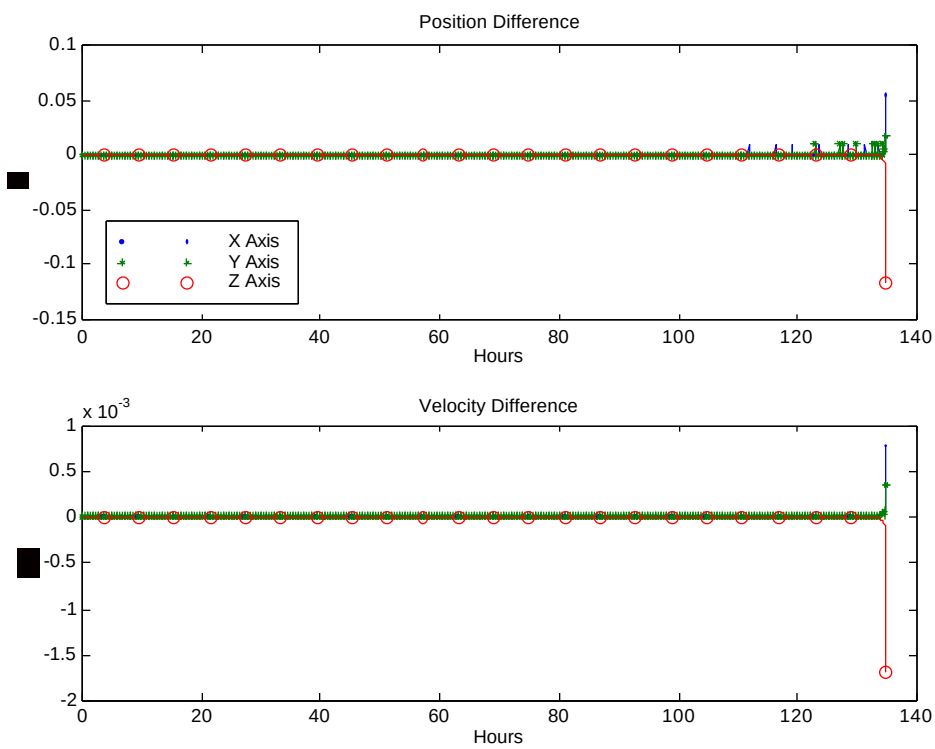

Figure 11. Position and Velocity Differences from Baseline: Cometary Gravitational Parameter, μ, Halved Over Baseline Value (Run #6)

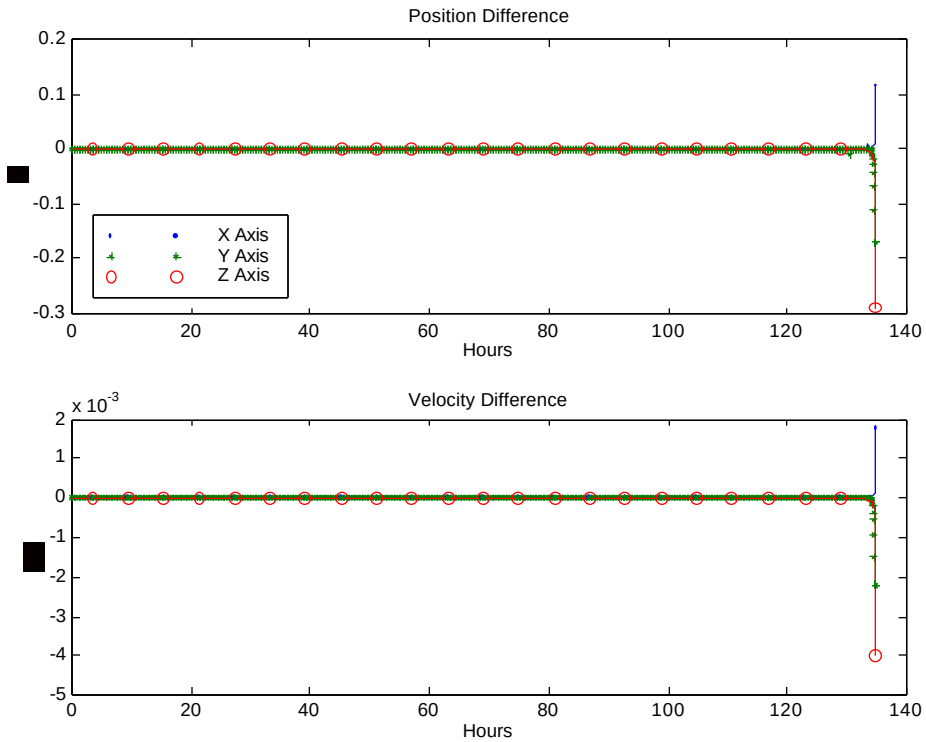

Figure 12. Position and Velocity Differences from Baseline: Rotating Cometary Nucleus, Baseline Position and Velocity Values (Run #7)

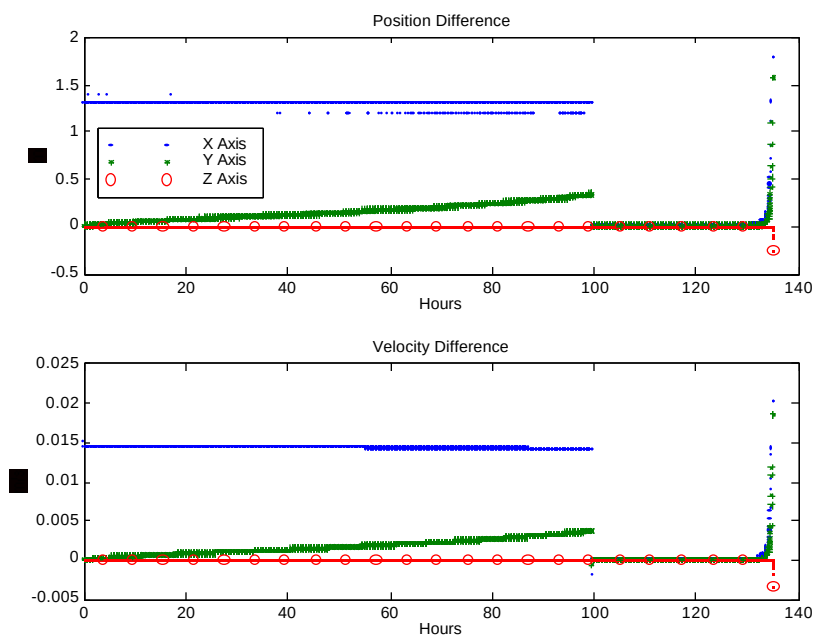

Figure 13. Position and Velocity Differences from Baseline: Atmosphere Enabled; Jet Flowing Along Nucleus' X-axis; Non-rotating Nucleus (Run #8)

Note: the spacecraft emerges from the jet after approximately 100 hours and corrects its course back to baseline

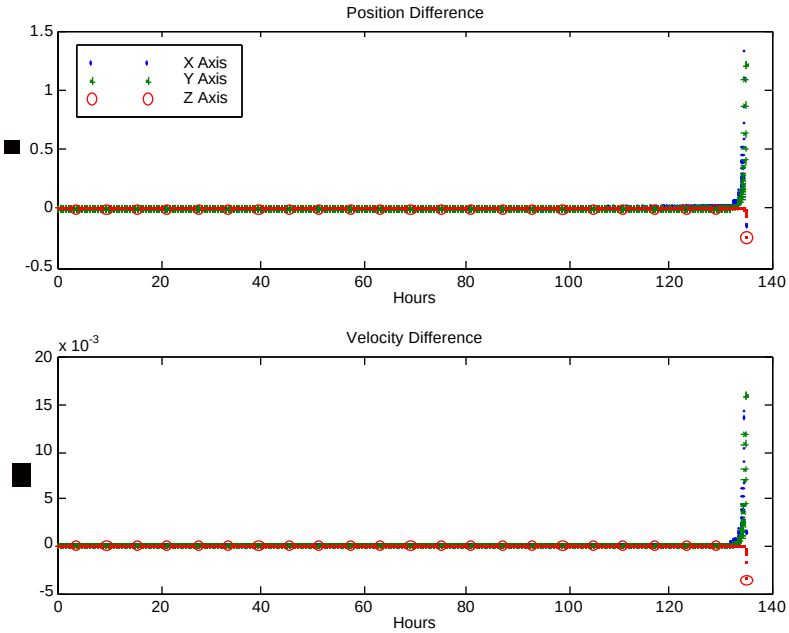

Figure 14. Position and Velocity Differences from Baseline: Atmosphere Enabled; Jet Flowing Along Y-axis. (Run #9)

Note: Spacecraft does not enter jet region until close to the end of the trajectory

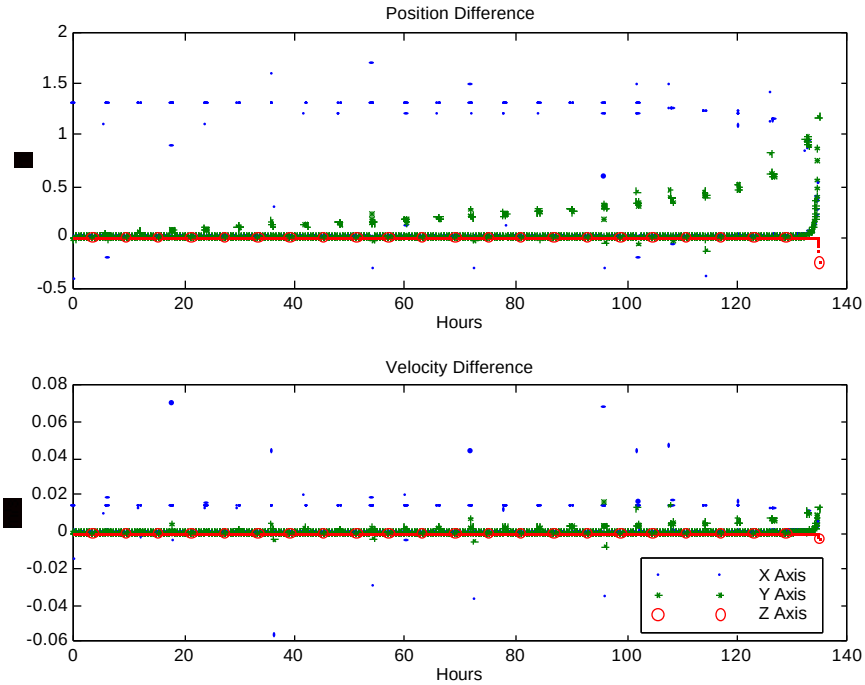

Figure 15. Position and Velocity Differences from Baseline: Atmosphere Enabled; Jet Aligned Along X-axis of Cometary Nucleus; Nucleus Rotating with a period of 6 hours. (Run #10)

Note: The spacecraft encounters the jet at discrete times along the trajectory – the controller works each time to correct the trajectory back to the desired baseline waypoints.

Given the encouraging results of the initial simulation, the same trajectory was used as the initial approach to the comet. Two more waypoints were added on the surface, at an approximation of where the ballistic trajectory would land. Putting two waypoints close together essentially allowed the controller to come to a stop at the desired landing site. The velocity of these waypoints was the rotational velocity of the surface of the comet at that point.

A baseline landing simulation was run using the parameters of the baseline approach simulation. The satellite touched down 2.83 m to the side of the targeted landing site. At touchdown the spacecraft had a normal velocity of 17.7 cm/s, and a tangential velocity of 5.1 cm/s.

Two more simulations were run using a rotating jet and atmosphere [Runs # 11 & 12], and using the second, more realistic gravity field. Addition of the rotating jet and atmosphere did not affect the landing site or velocities. Addition of the realistic gravity field moved the landing to 2.87 m from target, The normal velocity at touchdown was 16.7 cm/s, and the tangential velocity was 5.8 cm/s. The following figure, Figure 16, shows a close-up view of the landing of this trajectory.

The 'realistic modified' gravity field had all cross-terms reversed. Little difference between the two models should be expected since the trajectory took place in the comet's equatorial plane.

Table 5. Results of Landing Simulations for Various Perturbations

Baseline	No Atmosphere, No Jets, No Rotation, No offset in initial pos & vel	random gravity field	Distance Error 2.87 m	Velocity Error 0.18 m/s	ΔV used 1.83 m/s
Run #	**Perturbation from Baseline** *(in terms of initial position & velocity or comet characteristic)*	**Gravity Field 'Make-up'**	**Distance Offset from Baseline (m)**	**Velocity Offset from Baseline (m/s)**	**ΔV used (m/s)**
11	Rotating Jet and Atmosphere	'realistic'	0.04	0.01	7.92
12	Rotating Jet and Atmosphere	'realistic modified'	0.04	0.01	8.01

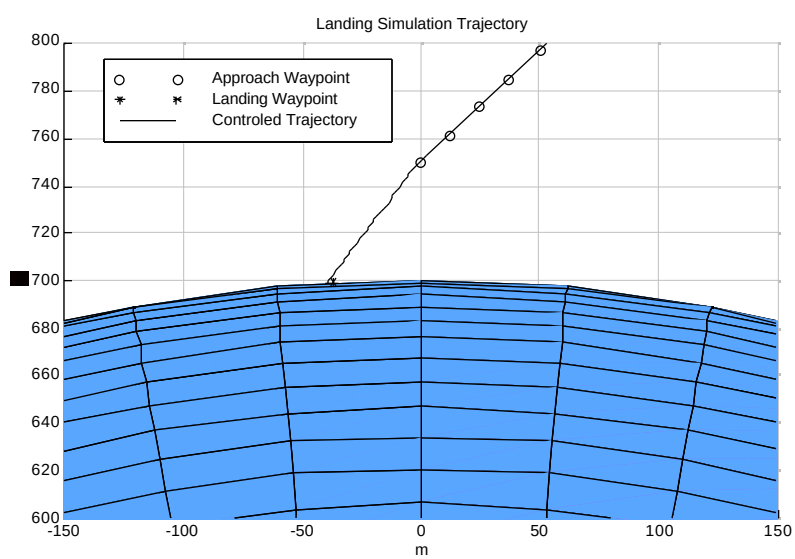

Figure 16 Close-up Of The Landing on a Rotating, Active Nucleus

CONCLUSION

Over the course of this study a simulation environment suitable for development of autonomous small-body landing control algorithms was implemented. This environment has at its core the Microcosm High Precision Orbit Propagator. This environment was used to implement an environmental model based on values from a survey of the literature on comet nuclei. The current state of the simulator makes some simplifying assumptions about the nature of the cometary body and atmosphere. These assumptions are valid for the preliminary nature of the study, but more advanced studies would require some refinement of these assumptions.

Future work could improve capabilities of the simulator for implementing more complicated models. Specifically the model for the continuous portion of the comet atmosphere, and the model for the jets could be improved over the current, simple exponential atmosphere and conical jet models. Also the models for the comet surface and rotation could be improved over the spherical assumptions made in this study.

The autonomous landing controller was able to perform controlled, soft landings under a variety of circumstances. Simulations performed included large initialization offsets, realistic and random gravity fields, rotating and non-rotating nuclei, and with and without jets. In all cases the control algorithms were able to maintain control of the vehicle and achieve the desired end state within a few meters position and m/s velocity. On the landing simulations the spacecraft set down within 3m of the intended target, and at under 20 cm/s vertical and 10 cm/s horizontal velocity. The controller used only a modicum of ΔV, which should be easily achieved by the spacecraft.

These results show the feasibility of autonomous controlled landings on small bodies. However, they must be taken as a qualitative and not quantitative results, the reason for this being the aforementioned simplifications to the environmental model and the lack of navigation errors and biases. The navigation errors could have a significant effect on the performance of the landing controller. Future work will estimate the potential errors of autonomous navigation around a cometary body and will implement these errors into the landing controller. The work will also refine the control algorithms to compensate for the additional errors.

This work should be quite applicable to anticipated near-term small-body missions such as Champollion/DS4, SpaceDev missions, and, eventually, landings on small moons orbiting other planets such as Phobos and Deimos.

ACKNOWLEDGMENTS

This work was funded under the NASA Phase I SBIR contract 07.02 9444[7] administered through the Jet Propulsion Laboratory. Dr. Fred Hadaegh at JPL was the technical monitor and his inputs and encouragement during the effort are appreciated.

REFERENCES

1. Möhlmann, D., “Comet 46 P/Wirtanen Nucleus Reference Model”, version 1(December 1996), DLR document ROL–DLR/Möh–TN 001/96.
2. Oria, A. J. & Bowling, T. S., “Orbit Perturbations in the vicinity of an active cometary nucleus”, *J. Planet. Space Sci*., Vol. 43, No. 12, pp. 1579–1585, 1995, Elsevier Science Ltd.
3. Klinger, J., et al., “Towards a model of cometary nuclei for engineering studies for future space missions to comets”, *J. Planet. Space Sci*., Vol. 44, No. 7, pp. 637–653, 1996, Elsevier Science Ltd.
4. Miller, J. K., et al., “Orbit Determination of the Comet Rendezvous/Asteroid Flyby Mission: Post-Rendezvous”, AIAA paper 89–0348, presented at the *AIAA 27th Aerospace Sciences Meeting*, January 9–12 1989, Reno, NV.

5. Long, A. C. et. al. (eds.), *Goddard Trajectory Determination System (GTDS) Mathematical Theory (Revision 1)*, FDD/552-89/0001 and CSC/TR-89/6001, NASA Goddard Space Flight Center and Computer Sciences Corporation, Greenbelt and Silver Spring, Maryland, pp. 3-14 to 3-16 (precession), 3-19 to 3-21 (nutation), 3-24 to 3-26 (diurnal rotation), 3-54 to 3-64 (Keplerian to Cartesian), 4-1 to 4-66 (force models), 1989.

6. Vallado, D. A., *Fundamentals of Astrodynamics and Applications*, McGraw-Hill, 1997.

7. Dawson, S., "Fast track Lunar/mars Autonomous Navigation & Orbit Control", *Microcosm internal document*, 97-1791, September, 1997.

Microcosm Internal Documents

M1. Dawson, S., "Cometary near-nucleus environment from an orbit control perspective", *Microcosm internal document*, 97–0767, April 8, 1997.

M2. Dawson, S., et al., "Terminal G&C for Planetary Landers: Salient Points", *Microcosm internal document*, 22 April 1997.

M3. Early, L. W., "Asteroid/Comet Force Models", *Microcosm internal document* , 97–1636, August 1 1997.

M4. Königsmann, H. J., "Comet Approach Controller", *Microcosm internal document*, 7/21/95.

M5. Königsmann, H. J., "How to find orbit controller gains", *Microcosm internal document*, 97–1659, August 6, 1997.